

DOI: <https://dx.doi.org/10.21123/bsj.2023.6842>

A Developed Colorimetric Assay Using Unmodified Gold Nanoparticles for the Identification of *Acinetobacter baumannii* Isolates from Different Clinical Samples

Mohamed M. Sehree*¹  Amani M. Al-Kaysi²  Hanaa N. Abdullah² 

¹College of Nursing, University of Telafer, Iraq.

²College of Health and Medical Technology, Middle Technical University, Iraq.

*Corresponding authors: mohamedshree@uotelafer.edu.iq

E-mail addresses: amanialkaesi@gmail.com , hanaa.naji@mtu.edu.iq

Received 15/12/2021, Revised 6/8/2022, Accepted 8/8/2022, Published Online First 20/1/2023,
Published 1/8/2023



This work is licensed under a [Creative Commons Attribution 4.0 International License](https://creativecommons.org/licenses/by/4.0/).

Abstract:

Acinetobacter baumannii (*A. baumannii*) is considered a critical healthcare problem for patients in intensive care units due to its high ability to be multidrug-resistant to most commercially available antibiotics. The aim of this study is to develop a colorimetric assay to quantitatively detect the target DNA of *A. baumannii* based on unmodified gold nanoparticles (AuNPs) from different clinical samples (burns, surgical wounds, sputum, blood and urine). A total of thirty-six *A. baumannii* clinical isolates were collected from five Iraqi hospitals in Erbil and Mosul provinces within the period from September 2020 to January 2021. Bacterial isolation and biochemical identification of isolates were carried out followed by DNA extraction from 36 isolates and six negative control ATCC strains (*Salmonella typhi*, *Escherichia coli*, *Klebsiella pneumoniae*, *Pseudomonas aeruginosa*, *Enterobacter aeruginosa*, *Staphylococcus aureus*) and only one positive control ATCC *A. baumannii* using Phenol/Chloroform method. AuNPs were synthesized using the citrate reduction method and examined by XDR, FTIR, UV-VIS, FE-SEM, and TEM. The optimized colorimetric assay was employed based on unmodified spherical AuNPs and PCR amplification of *16S rRNA* intergenic spacer sequences (ITS) with species-specific DNA oligo-targeters. Detection and optimization of *A. baumannii* amplicons using unmodified AuNPs were performed based on species-specific DNA oligonucleotide. The AuNPs assay was able to colorimetrically detect and distinguish *A. baumannii* from other ATCC bacterial isolates. The turnaround time of this assay was about 3 hours, including sample preparation and amplification, to show (0.025-6 ng μ l⁻¹) as a detection limit of DNA concentration. The efficacy of colorimetric detection was proved to effectively diagnose *A. baumannii* isolates with high sensitivity, simplicity, and robustness to rapidly diagnose *A. baumannii* isolates from different clinical samples.

Keywords: *Acinetobacter baumannii*, AuNPs, Colorimetric assay, *16S rRNA*, PCR

Introduction:

Acinetobacter baumannii has become a global health threat and burden, especially in hospitals. *Acinetobacter* species were found to be the reason behind a wide range of hospital-acquired infections such as nosocomial pneumonia, urinary tract infections, meningitis, septicemia, endocarditis, burn, and wound infections¹⁻³. *A. baumannii* is the most outstanding and virulent reason for bacterial pathogens, the infections which are caused by *A. baumannii* complex (ACB) predominantly referred to *A. baumannii* infections⁴. This bacterium has been involved with two crucial human pathogens;

firstly, it can survive on -alive and inert surfaces for a long time with high epidemic risks. Secondly, it is considered as one of the most multidrug-resistant microbes to many antibiotics such as carbapenems which probably leads to complicated medication issues⁵. It causes complicated cases that may lead to death. It has been noticed by the medical community that *A. baumannii* can develop new mechanisms to be resistant to other clinical effective medicines employed⁶.

Several studies have been reported by employing conventional biochemical tests and automated systems such as API20 E and Vitek GNI

card to detect *A. baumannii*⁷⁻⁹. However, these techniques encountered some challenges and were characterized by time-consuming, expensive, and semi-automatic methods that waste a significant amount of biological stuff^{8, 10}. Polymerase chain reaction (PCR), has a great ability to simplify, specify, diagnose, characterize and classify the type of bacterial infection¹¹. The genus of *Acinetobacter* was identified by employing PCR to analyze the gene *16S rRNA*⁷. Furthermore, PCR tools were robust to identify *Acinetobacter* species with high sensitivity. However, there are some challenges encountered by this technology which require high expense and effort, complicated laboratory equipment with highly experienced people^{11, 12}. It was obviously noticed that the biosynthesis method to prepare nanoparticles based on different materials such as silver and gold provided efficient ways to treat various diseases in biomedical applications^{13, 14}. Particularly, AuNPs was considered an effective metal against many pathogenic diseases and tumor cases¹⁵. Different methods based on chemical, physical, and biological materials were reported. Interestingly, it was reported that the biological methods to prepare AuNPs based on extracted stuff from plants such as phytochemicals can produce an easy and less toxic process¹⁶. Some publications found that biosynthesis based on AuNPs is more efficient against gram-negative bacteria compared to gram-positive bacterial strains, where gram positive possess a thick layer of peptidoglycan which has the ability to curb the AuNPs invasion¹⁷.

Gold nanoparticles (GNPs) were getting more commonly used than other metals, because of producing excellent biocompatible results with a high possibility to be employed in biology and medicine fields, easy functionalization on the surfaces, high solubility, strong scattering, and absorption with eco-friendly material¹⁸. The gold spherical nanoparticles diameters roughly ranged (2-100 nm), which reveals a wide range of spectra for bacterial detection¹⁰. The optical method which is used for bacterial pathogens detection based on NPs is classified into three techniques colorimetric, fluorescent, and nonlinear optical methods¹⁸. In the present work, there will be highlighting on the colorimetric assay to detect *A. baumannii* from different clinical samples based on AuNPs.

In 1996, the first application of bacterial detection based on gold NPs using a colorimetric method of target DNA was achieved¹⁹. Colorimetric assay can either be used for qualitative detection via naked eyes based on a target-induced

visual color change or quantitatively by depending on absorption measurement within the region of UV-Vis²⁰. Gold nanoparticles offer unique features called Localized Surface Plasmon Resonance (LSPR), which is responsible for the intensity of red color in solution. The red-to-blue color change depends on aggregated AuNPs, which allow for easily visible detection without supporting any other instruments. This chromatic change of solution comes from salt addition that grants a negative charge to the surface of AuNPs due to citrate ions reduction²¹.

Li and his colleagues studied the interactions of single (ss-DNA) and double-stranded DNA (ds-DNA) with AuNPs. It was observed that ss-DNA primers can be absorbed on the surface of unmodified AuNPs (negative charged) due to the attraction force with naked positive charged nitrogenous bases of ss-DNA²². Consequently, the primers will be restricted on the AuNPs surface, leading to aggregate the AuNPs and changing the colour solution to blue¹⁰. Whereas the repulsion phenomenon, which occurs with a negative charge phosphate backbone, will lead to preventing the absorption of ds-DNA on the surface of AuNPs²². In this case, it will allow for AuNPs to resist salt-induced aggregation with no red to blue colour change due to the presence of free ds-DNA primers¹⁰.

Materials and Methods: Bacterial Isolates

A total number of 36 *A. baumannii* isolates were recovered from 375 samples (burns, surgical wounds, sputum, blood and urine) at Intensive Care Unite (ICU) wards of three different hospitals in Erbil city (Emergency Management Centre (EMC), Par Hospital and Virkary Children's Educational hospitals) and two hospitals in Mosul city (Al-Jumhuri Teaching Hospital/Burns ward plastic Surgery and Al-Salam Teaching Hospital)/Iraq from September 2020 to January 2021. Those 36 isolates of *A. baumannii* were previously diagnosed by cultivation (Chromagar *Acinetobacter* media, MacConkey, and blood agars), and biochemical tests (Catalase, Oxidase, API20E, and VITEK[®] 2 system). These strains were employed to assess the ability of advanced detection. Seven references of ATCC strains have been used as controls, six of them are negative (other G^{-ve} and G^{+ve} bacteria) with only one positive as mentioned in Table 1.

Table 1. Types of ATCC strains that are used for *A. baumannii* detection as standard control strains.

Isolate /Strain	Sources	Name of the bacteria	Control
ATCC 19606	MDC	<i>A.baumannii</i>	Positive
ATCC 14028	MDC	<i>Salmonalle typhi</i>	Negative
ATCC 25922	MDC	<i>Escherichia coli</i>	Negative
ATCC 23495	MDC	<i>Klebsiella pneumonia</i>	Negative
ATCC 27853	MDC	<i>Pseudomonas aeruginosa</i>	Negative
ATCC 13048	MDC	<i>Enterobacter aeruginosa</i>	Negative
ATCC 43300	MDC	<i>Staphylococcus aureus</i>	Negative

DNA Extraction of *A. baumannii* and reference ATCC strain

DNA extraction for all 36 *A. baumannii* and 7 reference ATCC strains was achieved by using a manual method based on phenol/chloroform. Gel electrophoresis technique was carried out to confirm genomic DNA extraction of all isolates that showed clear bands. Then, it was stored in the refrigerator at 4°C²³. Bacterium-universal forward and reversed primers 5'-TTGTACACACCGCCCGTC-3'(18mer) and 5'-TTCGCCTTTCCTCACGGTA-3'(20mer) (Humanizing Genomics Macrogen, Korea) were used to amplify a DNA fragment of 23S-16S rRNA

intergenic gene spacer (ITS)¹² as observed in the Tables 2 and 3.

Table 2. The optimal reaction mixture of PCR for 16S rRNA gene.

Reagent (Conc.)	Volume (µl)
Master mix	20
DNA templates (50 ng/uL)	2
Primer forward (10 picoMol)	2
Primer reverse (10 picoMol)	2
MgCl ₂	0.5
Free nuclease D.W	23.5

Table 3. The optimum conditions of PCR thermocycling for ITS region.

Stage	Steps	Temp(°C)	Time	No. of cycles
First	Initial Denaturation	95	5 min	1
Second	I DNA Denaturation	94	30 sec	35
	II Primer annealing *	63	30 sec	
	III Extension	72	90 sec	
Third	Final Extension	72	5 min	1

* The optimum temperature (63 °C) at Primer annealing step.

The visualization of Amplicons was done in a 2 % agarose gel at 7volt/cm 1x TBE buffer for 45 min stained with ethidium bromide. Fine PCR Clean-up Kit (SSufine, USA) was employed to purify PCR products. Then, a UV-Vis spectrophotometer instrument (NanoDrop, Analytik Jena™ 844-00200-2, ThermoFisher Scientific Inc.) was utilized to determine the DNA concentration.

Preparation of Gold Nanoparticle

Spherical AuNPs were reduced to Au ions by trisodium citrate dehydrate. Firstly, it was prepared (0.03 mol/L) of HAuCl₄ solution by dissolving 1 g of HAuCl₄ salt in 100 ml of deionized water. Then, 0.8 ml of HAuCl₄ solution was added to 16 ml H₂O with magnetic stirring under reflux, followed by adding 2 ml of sodium citrate solution (1%) at a boiling degree. The mixed solution needs to stay boiling for 15 min and then cooled at room temperature. After that, filter the produced wine-red colored solution using a 0.45 Mm syringe filter to be transferred into a new glass bottle²⁴.

Characterization of Gold Nanoparticle

Some techniques were used to study the absorption spectra and morphological properties of AuNPs which are listed with procedures:

X-ray diffraction preparation samples

Gold Nanoparticles were analyzed by employing X-ray diffraction. This process involves the reduction of AuNPs solution by dropping it on the glass surface under low heating equipment. The fallen drops will dry gradually to cover the glass surface used for visualization at 40 KV voltage. And then, the AuNPs were investigated by running the X-ray instrument at the voltage of 20 mA with Cu K radiations²⁵.

Fourier Transform Infrared Spectroscopy (FTIR)

Fourier Transform Infrared measurements of AuNPs were achieved by using technology (IRAffinity-1-SHMADZU). This instrument can be used to measure the liquid and solid samples without preparation. FTIR scanning was achieved

within the range (500 - 4000 cm^{-1}).

Measurements of UV-Visible

Spectrophotometric measurements were achieved to confirm the wavelength scanning range of AuNPs by using a spectrophotometer instrument (UV-1900i, SHIMADZU, JAPAN). Absorbance measurements of the AuNPs were scanned within the range of (400–800 nm) region to find out the optimum wavelength¹².

Field Scanning Electron Microscopic (FSEM) sample preparation

The morphological features of AuNPs were studied under Field Scanning Electron Microscopic imaging (Inspect F 50 FE-SEM, USA). The frozen and dried sample of synthesized AuNPs was sonicated with an ultrasonic instrument. The sample was basically prepared by placing a small drop of AuNPs solution on the clean glass slide to dry using the oven with kind heating gradually. The dried samples were transferred onto FESEM alumina supports and sputtered with gold by a coater of Blazers. The photographs were picked up under a range (14-10⁶X) magnification and a width 19.9 mm^{26} .

Transmission Electron Microscope (TEM)

The morphology and size of gold nanoparticles were characterized by considering TEM technology. The procedure was carried out by spreading one drop of GNPs suspension onto carbon-coated TEM copper grids. Then, a Tecnai G2 Spirit transmission electron microscope equipped with a BioTwin lens configuration (TEM Carl Zeiss EM10C-100Kv-Germany) was employed by applying 80 kV of accelerating voltage²⁷.

Colorimetric detection of *A. baumannii* isolates

Colorimetric detection of *A. baumannii* based on unmodified spherical AuNPs and Amplicon of ITS region DNA was carried out. Sequencing detection includes adding 1 μL of Amplicon product to 2 μL of hybridization buffer. This buffer consists of two oligo-targeters (specific targets sequence), the first one is (ACB 5'-GACTGGTTGAAGTTATAGA-TAAAAGAT-3') used for genus, and another one is (ACI 5'-AATTCATATACCAAACGCTCGATTC-3') utilized for species²⁸. The mixture of reaction consists of (0.3 $\mu\text{mol.l}^{-1}$ oligotargeters, 1.3 mmol l^{-1} phosphate buffer (pH 7.4), and 15 mmol l^{-1} NaCl) were added to each other. The Denaturation occurs when the mixture reaction is heated for 3 min at 95 °C, followed by cooling the reaction to 50 °C for 1 min annealing. After that, 200 μL of AuNPs was

added where the images would be picked up when changing the color from red to blue for 10 min. The scanning process was done for each sample using a spectrophotometer (UV-Vis) within the wavelengths of (400 to 800nm)¹².

Optimal AuNPs prototype assay of *A. baumannii* detection

A series of various DNA target concentrations were prepared from (0.01-15 $\text{ng}\mu\text{l}^{-1}$), 1 μL was taken from each concentration to be individually mixed with 2 μL of hybridization buffer 1.3 mmol l^{-1} pbs (pH7.4), 15 mmol l^{-1} NaCl and various concentrations of oligotargeter (0.5-7 $\text{pmol/}\mu\text{L}$). The mixed solutions were heated to 95 °C for denaturation event for 3 min and then decreased the temperature to 50 °C for the annealing step for 1 min. After that, 200 μL of AuNPs were added to the mixture. The color solution would change from red to blue as a result of AuNPs aggregation. Different responses of mixture solutions have been determined at various wavelengths ranging from 400-800 nm to find out the highest reading. The same process was done with negative control by adding only 2 μL of *Salmonella typhi* DNA (ATCC) to be mixed with 2 μL hybridization buffer²⁹.

Statistical Analysis

In the current study, analysis of the size distribution of the prepared AuNPs was measured by Java-based image processing program. Moreover, the results of Absorbances were statistically analyzed based on Excel to show the Absorbance ratio (A610/A520) of Colorimetric responses of *A. baumannii* based on AuNPs protocol and optimum concentrations of both NaCl and DNA.

Results and Discussions:

Result

In the current study, one positive control (ATCC 19606) of *A. baumannii* was employed as a reference strain, while 6 negative controls belong to different bacterial strains (ATCC 14028, ATCC 25922, ATCC 23495, ATCC 27853, ATCC 13048, and ATCC 43300) were utilized. Those 36 isolates of *A. baumannii* were previously diagnosed using different strategies such as conventional methods, cultivation, biochemical tests, API20E, and VITEK® 2 system. Furthermore, all *A. baumannii* strains have been identified by the molecular method based on the amplification of the *16S rRNA* ITS region using universal primers and gel electrophoresis, size of amplicon (1242 bp) as observed in Fig. 1.

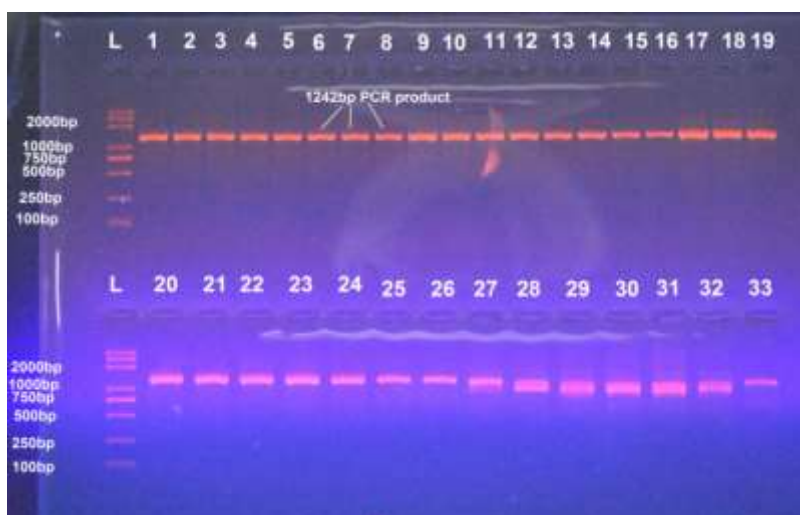


Figure 1. Electrophoresis of PCR product (clean up) of *16S rRNA* on Agarose gel (2%) for 45 min at 7 volt/cm, 1242bp. Lane 1-26: *A. baumannii* isolates with ATCC; Lane (27) *S. typhi*; Lane (28) *E. aerogenes*; Lane (29) *P. aeruginosa*; Lane (30) *E. coli*; Lane (31) *K. pneumonia*; Lane (32): *S. aureus* (33) respectively.

Characterization of AuNPs

In this study, different characterization methods were used to confirm AuNPs by:

XRD:

The first technique was used to investigate gold nanoparticle sizes. Four different peaks of gold nanoparticle diffraction pattern with Miller Index

were obtained at 2 Theta (2θ) values scale 38.25, 44.35, 64.5, and 77.07. These peaks are respectively compatible with the (111), (200), (220), and (311) sets of lattice planes, observed and indexed to the face-centred cubic structures for gold to produce the same database of some publications^{30, 31} as shown in Fig. 2.

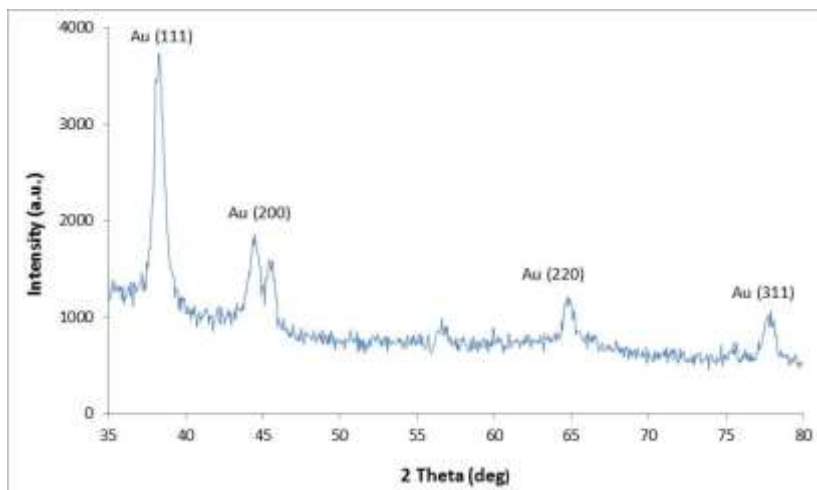


Figure 2. X-ray diffraction (XDR) analysis of synthetic AuNps by Tri-sodium citrate

RD was successfully achieved to produce four peaks, as noticed in Fig. 2 above. In the current study, a peak at 38.2° attributed to the (111) diffraction plane of Au. This peak confirms the formation of crystalline Au in the face-centered cubic structure corresponding with JCPDS# 04-0784. The appearance of the high intensity peak (111) comes as a result of adding more AuNps in the solution compared with other peaks that hold (200), (220), and (311) that produced poor spectra less than one. All intensities are assigned to

diffraction peaks of gold metal. The current results were relatively identical with a previous study that reported three peaks of AuNps (111), (200), and (220) produced by the XRD technique^{32, 33}.

However, it was demonstrated that the diffraction of gold nanoparticles products is not entirely pure, despite the appearance of the diffraction pattern. The present finding supports the author's study, which reported that the AuNPs peaks are not completely pure³⁴.

FTIR:

This technique is an indication of the absorption bands for the characterization of Gold (NPs) which were prepared by tri-sodium citrate. The results have shown a high intensity of AuNPs at 524 cm^{-1} . Moreover, two strong bands at different intensities were shown, the sharp band was

noticed at 1612 cm^{-1} is related to (C=C) stretching vibrations, while the broad band which has been observed at 3244 cm^{-1} is assigned to O-H stretching vibrations as explained in Fig. 3.

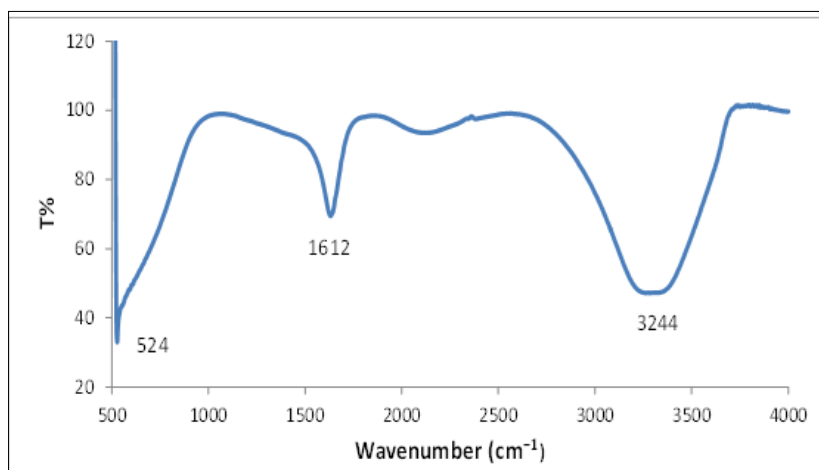


Figure 3. Fourier Transform Infrared Spectroscopy (FTIR) analysis spectra for AuNPs chemically synthesized

FTIR results that are mentioned in Fig. 3 are relatively compatible with the FTIR analysis that was reported by Moghaddam and co-workers to reveal the intensities 577, 1641, and 3416 cm^{-1} that are related to AuNPs, (C=C) and O-H stretching vibrations respectively ³⁵.

UV-Vis:

Another technique was carried out to investigate the optical features of synthesized

AuNPs using UV-Vis spectroscopy within the range of wavelength 400-800 nm. The reduction of HAuCl_4 to AuNPs has been successfully confirmed due to observing the color change of the reaction mixture from yellow to red ³¹. In the present work, a sharp absorption peak of Gold-NPs at 521 nm was noticed, which is known as Surface Plasmon Resonance (SPR) as shown in Fig. 4.

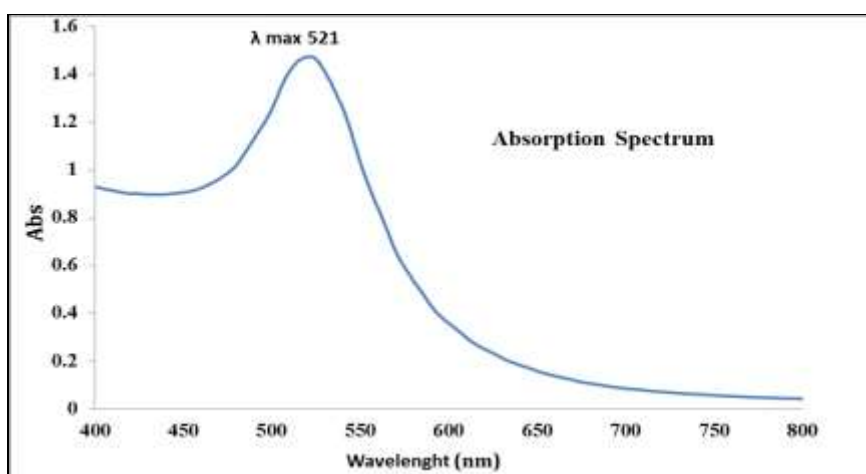


Figure 0. UV-Vis of maximum absorption spectrum of synthesized AuPNs

In the UV-VIS technique, a maximum response was produced at 521 nm as a result of HAuCl_4 reduction by Tri sodium citrate to form AuNPs to significantly correspond with the surface plasmon resonance (SPR) band as shown in Fig. 4.

The current findings were significantly compatible with the recent paper that reported a strong response (SPR) of Gold-NPs at 520 nm as a result of the yellow to red color change ²⁷.

FE-SEM:

The morphology of synthesized AuNPs was studied using (Inspect F50 FE-SEM) technology under magnification (130000X) and working different sizes ranging 15-24 nm. The present data

showed much finer AuNPs when compared with another study conducted in 2013, Gold-NPs were measured by SEM that showed particles in spherical morphology within the size range of 53-67 nm with few aggregations³⁰ as shown in Fig. 5.

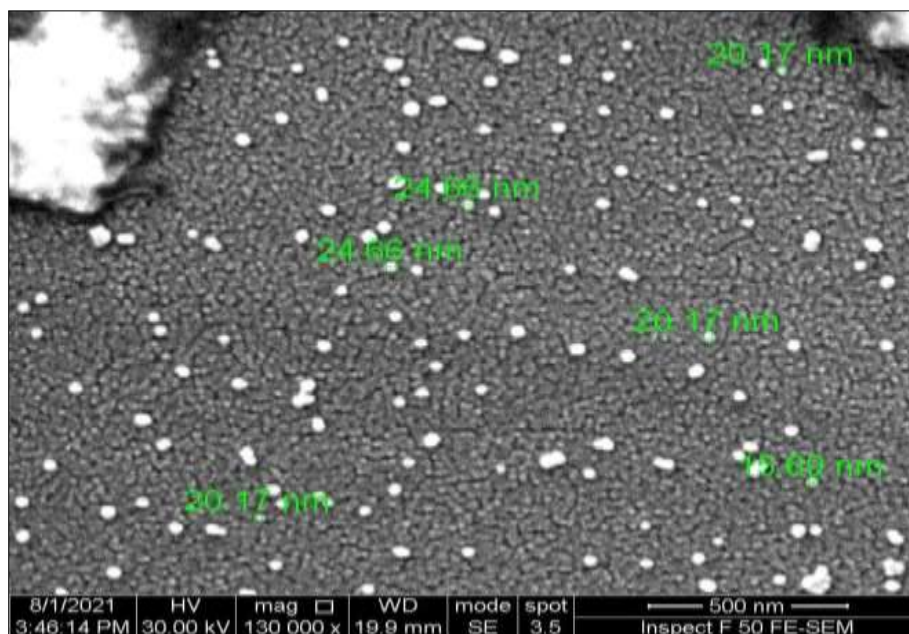


Figure 5. Field emission scanning electron microscopy (FE-SEM) image showing the spherical morphology of gold nanoparticles.

The present data showed finer AuNPs when compared with another study conducted in 2013, gold-NPs were measured by SEM that showed particles in spherical morphology within the size range of 53-67 nm with few aggregations³⁰.

TEM:

This technology was employed to check the morphological features of AuNPs, including shape and size under different magnifications 21,560, 60,000, and 100,000 KX respectively. The

micrographs refer that AuNPs were spherical in shapes, uniform distribution with few aggregated particles. The mean of gold particles size was measured to be 17.48 ± 2 nm using a Java-based image processing program, which supports FE-SEM results as observed in Fig. 6. The characteristics of GNPs in the current study were relatively compatible with the findings of another recent publication, which was performed in 2021, that revealed spherical shapes with an average particle size of 22.18 ± 2 nm²⁷.

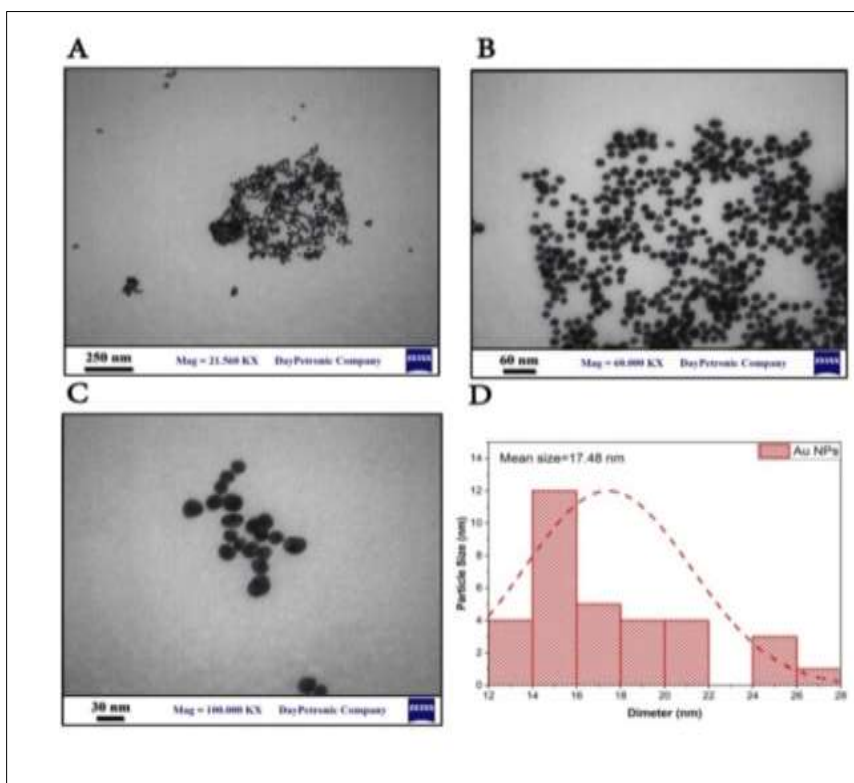


Figure 6. Transmission Electron Microscope (TEM) Characterization of gold nanoparticles (GNPs) under different magnifications (A) 21,560KX, (B) 60,000KX, (C) 100,000KX, and (D) Analysis of the size distribution of the prepared AuNPs measured by Java-based image processing program.

Optimization of Colorimetric assay

The color solution of colloidal gold-NPs is significantly influenced by some major parameters: Phosphate buffer saline PBS, AuNPs, primer concentrations, and temperature²⁹. However, in the present, it was observed that two other factors had a significant effect on the color change of AuNPs, such as buffer and target DNA concentrations. *A. baumannii* isolates were investigated using the

colorimetric technique with positive and negative controls (ATCC) were equivalently employed. The positive and negative controls were compared with each other to observe different colors. The negative control created a sharp response at 520 nm with no color change (red), while the positive control produced an abroad absorption peak shifting at 610 nm with red to blue color change as seen in Fig. 7.

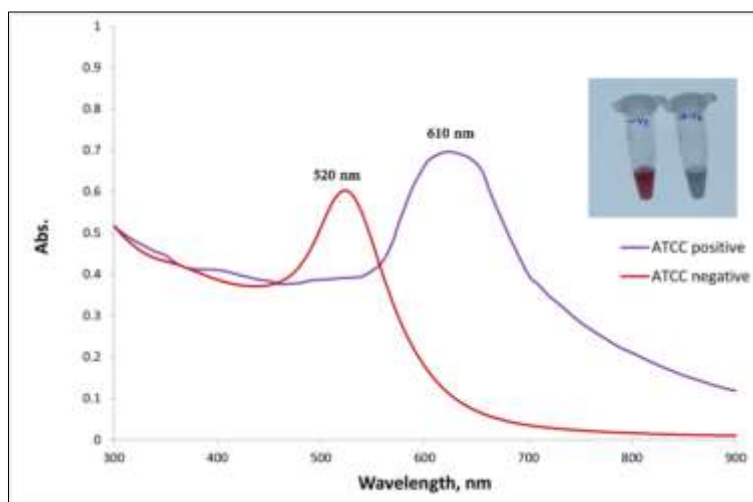


Figure 7. The absorption peaks of (ATCC) including negative (*Salmonella typhi* 14028) and positive (*A. baumannii* 19606) samples that showed (non-aggregated AuNPs; red) at 520 nm and (aggregated AuNPs; blue) at 610 nm respectively.

The surfaces of AuNPs were covered with citrate anions (negative charges). These anions have no ability to aggregate the nanoparticles, the red color stays with no change. Salt (NaCl) increases the growth of nanoparticle clusters, leading to shifting in color from red to blue. In the current study, the optimum concentration of NaCl was examined to be 200 mmol l⁻¹ to produce a response at 610 nm a color change to blue as explained in Fig. 8.

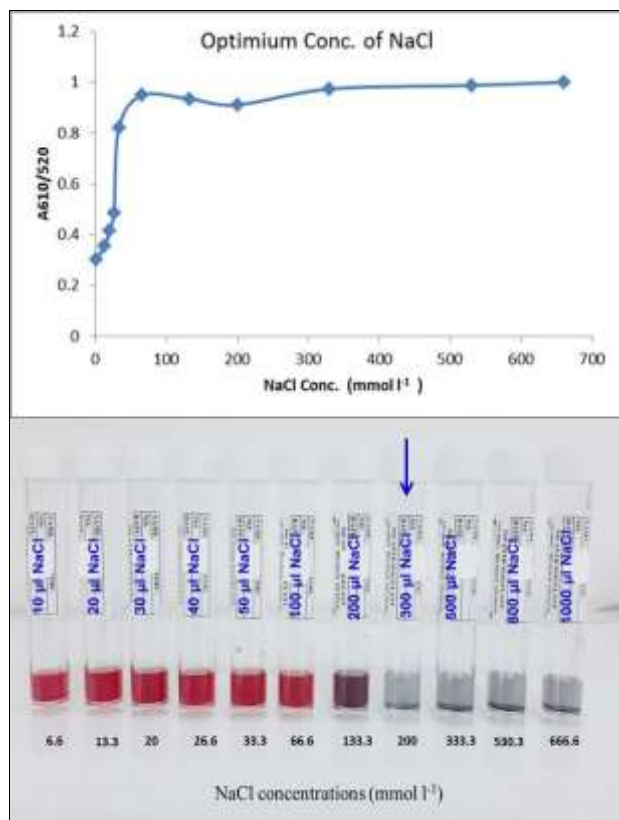


Figure 8. Investigation different concentrations of NaCl ranged from 6.6, 13.3, 20, 26.6, 33.3, 66.6, 133.3, 200, 333.3, 530.3, 666.6 mmol l⁻¹, to find out the optimal concentration that leads to red to blue color change.

In the AuNPs protocol, various concentrations of ss-DNA 0.025, 0.15, 0.3, 0.9, 1.5, 3, and 6 ng μ l⁻¹, have been investigated, and then compared with ds-DNA as a negative control to determine the detection concentration of ss-DNA added that ranged 0.025-6 ng μ l⁻¹ as noticed in Fig. 9.

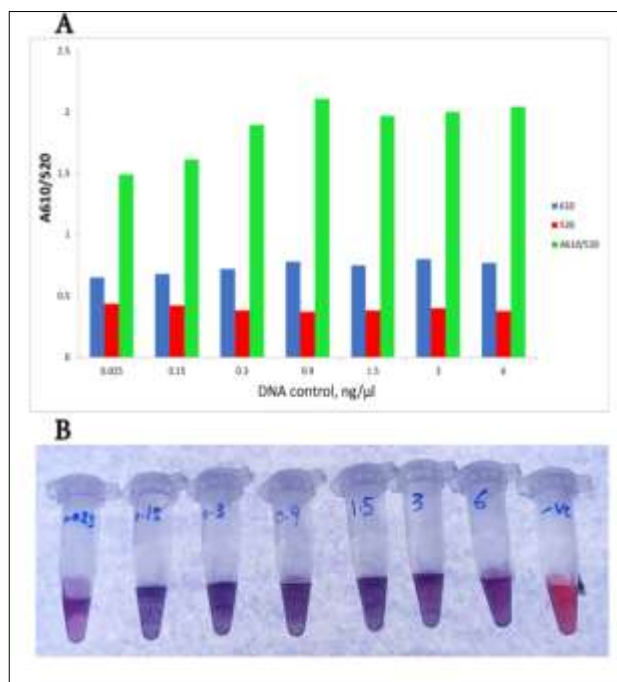


Figure 9. (A) The colorimetric responses of AuNPs solution with ssDNAs at absorbance ratio (A610/A520) (B) Nano-gold assay detection limit of *A. baumannii* PCR amplicon ATCC 19606 ranged 0.025 - 6 ng μ l⁻¹ compared with the negative control *Salmonella typhi* ATCC 14028 .

Interestingly, the absorbance ratio (A 610 /A 520) nm was employed to assess the aggregation degree of AuNPs in the solution. The low value of ratio refers to the dispersion of AuNPs; however, the high ratio indicates that gold NPs have been aggregated well in the solution. As a result, the optimal concentration of PCR amplicon to achieve high GNPs aggregation is 0.9 ng μ l⁻¹ . The present results showed a high agreement with Yang *et al.* interpretation³⁶.

All isolates that were already identified as positive, were investigated with positive and negative ATCC controls based on AuNPs protocol. Those isolates produced a shift in response at 610 nm with red to blue or purple color change. In contrast, different strains of ATCC negative samples were tested to produce an absorption band at 520 nm with no color change (red), as observed in Fig. 10: A, B and C.

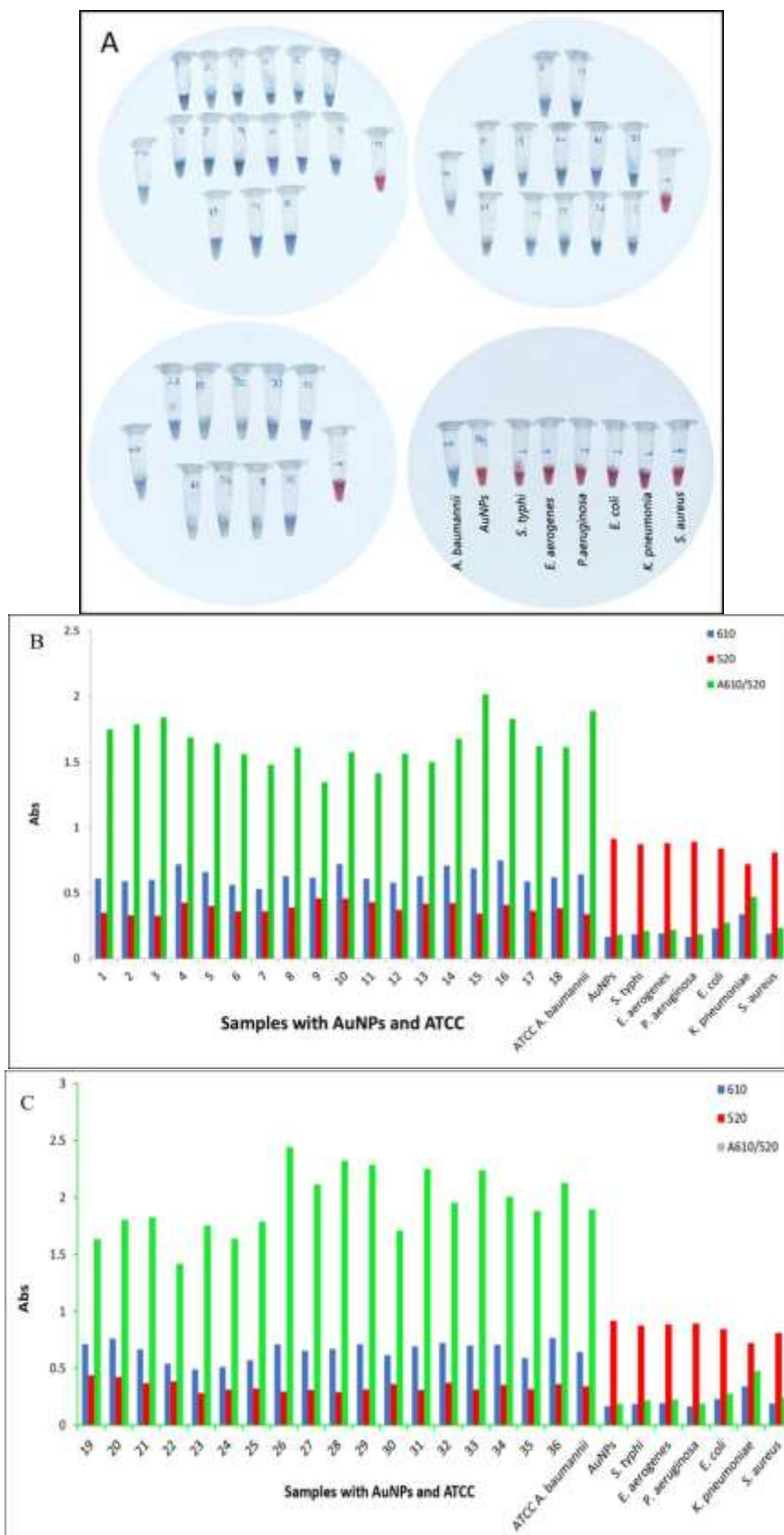


Figure 10. Colorimetric detection of *A. baumannii* isolates (1-36) with positive ATCC (*A.baumannii*), AuNPs blank and negative ATCC (*S. typhi*, *E. aerogenes*, *P.aeruginosa*, *E. coli*, *K. pneumoniae*, *S. aureus*). (A) Photographs of AuNPs solutions in the presence of ssDNA with species-specific Oligotargeters. (B and C) Absorbance ratio (A610/A520) show Colorimetric responses of *A. baumannii* based on AuNPs protocol.

Discussion:

Many recent papers have been reported by employing conventional biochemical tests, API20 E and automated VITEK®2 GNI card to detect *A. baumannii*^{8, 9, 37}. However, these techniques encountered some difficulties such as time-consuming, expensive, and semi-automatic techniques to waste large amounts of biological reagents^{8, 10}. In the current study, all 36 isolates of *A. baumannii* were previously diagnosed using different strategies such as conventional methods, cultivation, biochemical tests, API 20E, and VITEK® 2 systems. Another technique was employed to identify those isolates utilizing the molecular method. This technique was based on the amplification of the *16S rRNA* ITS region using universal primers and gel electrophoresis, size of amplicon 1242 bp with only one positive control (ATCC 19606) of *A. baumannii* as a reference strain, while 6 negative controls that belong to different bacterial strains (ATCC 14028, ATCC 25922, ATCC 23495, ATCC 27853, ATCC 13048, and ATCC 43300) were utilized as shown in Fig. 1.

The internal transcribed spacer (ITS) region was considered a known region to characterize different bacterial species. Genus and species-specific oligotargeters were used by Ko and co-workers to recognize the ITS region of *Acinetobacter* complex²⁸.

The previous results of PCR showed an accurate confirmation that all *Acinetobacter* species whose conventionally diagnosed were indeed *A. baumannii* based on the *16S rRNA*³⁸. Furthermore, specific oligo-targeters of *Acinetobacter* spp was employed to identify the ITS region which is a typical fingerprint of bacterial isolates recognition.

The principle of this method is to identify *A. baumannii* based on AuNPs by extracting DNA from bacterial colonies. After the amplification of DNA, the oligotargeters were used to detect PCR products based on unmodified spherical GNPs. Several parameters such as size, shape, and temperature of GNPs, as well as oligotargeters and salt concentration, have a direct influence on the GNPs assay¹². Therefore, these factors were carefully optimized to obtain the best results. In the present work, the denaturation step was carried out, the PCR products were heated up to 95°C for 3 minutes to break the hydrogen bonds and split the dsDNA to ssDNA. Then, the reaction was cooled at 55 °C for 1 minute annealing to enable ssDNA binding with oligotargeters. These steps were compared with another publication to show a high consistency by using 94-96 °C to denaturation the Amplicon, followed by decreasing the temperature to the range of 45-60 °C at the annealing step³⁹.

After that, 200 µL of AuNPs was added to stabilize the ssDNA primers in the colloidal solution to stop salt-induced clustering. In general, the amplicon (ssDNA) has a significant absorption on the surface of AuNPs compared with dsDNA. Consequently, the coated AuNPs with ssDNA are becoming more stable compared with uncoated Gold, this interpretation showed a high agreement with another study⁴⁰.

The primers combine with the complementary DNA sequence in the target-present (positive sample), leading to aggregation after adding the AuNPs in the presence of salt in hybridization buffer to obtain a signal shifted at 610 nm with red to blue color change. While the ssDNA primers remain with no binding in the case of DNA target absence that leads to stabilizing AuNPs and preventing the aggregation by the salt to produce a peak at 520 nm with no change color from red to blue. These steps were compatible with the procedure performed by an Arabian study in Qatar that shows a color change from red to blue¹⁰. The detection range of DNA Amplicon was carried out to be 0.025-6 ngµl⁻¹. The optimal concentration was chosen for DNA to be 0.9, which revealed a higher aggregation of AuNPs. The current study showed higher sensitivity compared with the detection limit of a published paper (0.4-13 ngµl⁻¹)¹².

It was noticed that the absorbance of positive samples and ATCC *A. baumannii* at 520 nm revealed low values compared with the increased responses at 610 nm to show high ratios (A610/A520) due to color change to blue. In contrast, the intensities of negative samples (AuNPs Blank and ATCC) showed higher values at 520 nm compared with 610 nm that produced low values leading to lower ratios (A610/ A520) nm due to no shifted occurrence with no color change (red) as shown in Fig. 7. The high ratios (A610/A520) indicate the significant aggregation of AuNPs compared to the lower ones that attribute to weak AuNPs clustering in the solution. These data revealed high compatibility with the recent research that was done in 2018³⁶. Accordingly, the ratio (A610/ A520) was employed as a function of quantitative determination of target DNA concentration in the mixture solution. These findings were highly consistent with a previous study, which reported that an absorbance peak ratio at 610 nm and 520 nm could be effectively employed to detect the concentration of DNA target⁴¹.

Conclusion:

In conclusion, an eco-friendly strategy was employed to prepare AuNPs based on trisodium citrate, described as a reducing and non-dispersive agent that resists the change in pH solution. In the current research, different characterization techniques, XDR, FTIR, UV-VIS, FE-SEM, and TEM, are employed. However, TEM, FE-SEM, and UV-Vis have efficiently been considered the most common characterization methods. Both TEM and FE-SEM provide high-resolution images for better understanding to measure AuNPs features such as particle size distribution and spherical morphology. Furthermore, UV-Vis is used to study the absorption peaks of AuNPs shifted in SPR and gain more information about conjugation and aggregation. AuNPs are successfully prepared and detected using a colorimetric assay by showing a sharp intensity at 610 nm due to the color change from red to blue. AuNPs is an interesting metal to be more commonly used for bacterial detection by many researchers than other metals, due to their high stability, optical features, high biocompatibility, and ease of surface functionalization. Consequently, the colorimetric assay based on AuNPs is characterized as sensitive, simple, rapid, robust, and inexpensive that had a high potential to diagnose *A. baumannii* from different samples compared to conventional methods.

Authors' declaration:

- Conflicts of Interest: None.
- I hereby confirm that all the Figures and Tables in the manuscript are mine. Besides, the Figures and images, which are not mine, have been given the permission for re-publication attached with the manuscript.
- Ethical Clearance: The project was approved by the local ethical committee at the College of Nursing, University of Telafer.

Authors' contribution:

Each of authors contribute develop the diagnosis of *A. baumannii*, and the work distributed as fellow : Sehree and Al-Kaysi prepare gold nanoparticles, Sehree and Abdullah employed optimized colorimetric assay based on unmodified spherical AuNPs and PCR amplification of *16S rRNA* intergenic spacer sequences (ITS) with species-specific DNA oligo-targeters of *A. baumannii*.

References:

1. Liu YM, Lee YT, Kuo SC, Chen TL, Liu CP, Liu CE. Comparison between bacteremia caused by *Acinetobacter pittii* and *Acinetobacter nosocomialis*. J Microbiol Immunol Infect., 2017 Feb 1; 50(1): 62-7.
2. Hamzah AS. Genotyping of *fusA* Gene from Clinical Isolates *Acinetobacter baumannii* in Baghdad. Baghdad Sci J. 2018; 15 (1):726-732
3. Ahmad NH, Mohammad GA. Identification of *Acinetobacter baumannii* and Determination of MDR and XDR Strains. Baghdad Sci J. 2020 Sep 1;17(3): 726-732
4. Fitzpatrick MA, Ozer EA, Hauser AR. Utility of whole-genome sequencing in characterizing *Acinetobacter* epidemiology and analyzing hospital outbreaks. J Clin. Microbiol., 2016 Mar; 54(3): 593-612.
5. Martín-Aspas A, Guerrero-Sánchez FM, García-Colchero F, Rodríguez-Roca S, Girón-González JA. Differential characteristics of *Acinetobacter baumannii* colonization and infection: risk factors, clinical picture, and mortality. Infect Drug Resist., 2018;11:861.
6. Gellings PS, Wilkins AA, Morici LA. Recent advances in the pursuit of an effective *Acinetobacter baumannii* vaccine. Path. 2020 Dec 19; 9(12): 1066.
7. Abdul-Hussein TM, Saadedin SM, Almaali HM, Al-Wattar WM. Evaluation of the phenotypic and genotypic detection of *Acinetobacter baumannii* isolated from Baghdad hospitals. Plant Arch. 2019; 19(2): 3801-4.
8. Vijayakumar S, Biswas I, Veeraraghavan B. Accurate identification of clinically important *Acinetobacter* spp.: an update. Futur Sci OA. 2019 Jun 27; 5(7): FSO395.
9. Bagudo AI, Obande GA, Harun A, Singh KK. Advances in automated techniques to identify complex . Asian Biomed. 2020 Oct 1; 14(5): 177-86.
10. Al-Saadi TM. gold nanoparticles-based assays for direct and cost effective detection of *clostridium difficile* in Qatar. M.SC [dissertation]. Qatar; College of Art and Sciences Qatar University; 2015.
11. Shahi S, Vahed SZ, Fathi N, Sharifi S. Polymerase chain reaction (PCR)-based methods: promising molecular tools in dentistry. Int J Biol Macromol. 2018 Oct 1; 117: 983-92.
12. Khalil MA, Azzazy HM, Attia AS, Hashem AG. A sensitive colorimetric assay for identification of *Acinetobacter baumannii* using unmodified gold nanoparticles. J Appl Microbiol. 2014 Aug; 117(2): 465-71.
13. Sathishkumar P, Vennila K, Jayakumar R, Yusoff AR, Hadibarata T, Palvannan T. Phyto-synthesis of silver nanoparticles using *Alternanthera tenella* leaf extract: An effective inhibitor for the migration of human breast adenocarcinoma (MCF-7) cells. Bioprocess Biosyst Eng. 2016 Apr; 39(4): 651-9.
14. Ban DK, Paul S. Functionalized gold and silver nanoparticles modulate amyloid fibrillation, defibrillation and cytotoxicity of lysozyme via altering protein surface character. Appl Surf Sci. 2019 Apr 15; (473): 373-85.
15. Sathishkumar P, Gu FL, Zhan Q, Palvannan T, Yusoff AR. Flavonoids mediated 'Green' nanomaterials: A novel nanomedicine system

- to treat various diseases—Current trends and future perspective. *Mater. Lett.* 2018 Jan 1; (210): 26-30.
16. Alsamhary K, Al-Enazi N, Alshehri WA, Ameen F. Gold nanoparticles synthesised by flavonoid tricetin as a potential antibacterial nanomedicine to treat respiratory infections causing opportunistic bacterial pathogens. *Microb.Pathog.* 2020 Feb 1; (139): 103928.
 17. Katas H, Lim CS, Azlan AY, Buang F, Busra MF. Antibacterial activity of biosynthesized gold nanoparticles using biomolecules from *Lignosus rhinocerotis* and chitosan. *Saudi Pharm J.* 2019 Feb 1; 27(2): 283-92.
 18. Yuan P, Ding X, Yang YY, Xu QH. Metal nanoparticles for diagnosis and therapy of bacterial infection. *Adv Healthc Mater.* 2018 Jul; 7(13): 1701392.
 19. Mirkin CA, Letsinger RL, Mucic RC, Storhoff JJ. A DNA-based method for rationally assembling nanoparticles into macroscopic materials. *Nature.* 1996 Aug; 382(6592): 6079.
 20. Xia N, Deng D, Wang Y, Fang C, Li SJ. Gold nanoparticle-based colorimetric method for the detection of prostate-specific antigen. *Int. J. Nanomedicine.* 2018; 13: 2521.
 21. Syed MA. Advances in nanodiagnostic techniques for microbial agents. *Biosens Bioelectron.* 2014 Jan 15; (51): 391-400.
 22. Li H, Rothberg L. Colorimetric detection of DNA sequences based on electrostatic interactions with unmodified gold nanoparticles. *Proc Natl Acad Sci U S A.* 2004 Sep 28; 101(39): 14036-9.
 23. Cheng HR, Jiang N. Extremely rapid extraction of DNA from bacteria and yeasts. *Biotechnol. Lett.* 2006 Jan; 28(1): 55-9.
 24. Sato K, Hosokawa K, Maeda M. Rapid aggregation of gold nanoparticles induced by non-cross-linking DNA hybridization. *J Am Chem Soc.* 2003 Jul 9; 125(27): 8102-3.
 25. Menon S, Rajeshkumar S, Kumar V. A review on biogenic synthesis of gold nanoparticles, characterization, and its applications. *Resour Technol.* 2017 Dec 1; 3(4): 516-27.
 26. Alam N, Sarkar M, Chowdhury T, Ghosh D, Chattopadhyay B. Characterization of a novel MDH1 bacterium from a virgin hot spring applicable for gold nanoparticle (GNPs) synthesis. *Adv Microbiol.* 2016; 6(09): 724.
 27. Al Saqr A, Khafagy ES, Alalaiwe A, Aldawsari MF, Alshahrani SM, Anwer MK, et al. . Synthesis of gold nanoparticles by using green machinery: Characterization and in vitro toxicity. *Nanomater Artic.* 2021 Mar 22; 11(3): 808.
 28. Ko WC, Lee NY, Su SC, Dijkshoorn L, Vaneechoutte M, Wang LR, et al. Oligonucleotide array-based identification of species in the *Acinetobacter calcoaceticus*-*A. baumannii* complex in isolates from blood cultures and antimicrobial susceptibility testing of the isolates. *J Clin Microbiol.* 2008 Jun; 46(6): 2052-9.
 29. Shawky SM, Bald D, Azzazy HM. Direct detection of unamplified hepatitis C virus RNA using unmodified gold nanoparticles. *Clin Biochem.* 2010 Sep 1; 43(13-14): 1163-8.
 30. Singh M, Kalaivani R, Manikandan S, Sangeetha N, Kumaraguru AK. Facile green synthesis of variable metallic gold nanoparticle using *Padina gymnospora*, a brown marine macroalga. *Appl Nanosci.* 2013 Apr; 3(2): 145-51.
 31. Mahdi HS, Parveen A. Biosynthesis, Characterization and antibacterial activity of gold nanoparticles (Au-NPs) using black lemon extract. *Mater Today Proc.* 2019 Jan 1; 18: 5164-9.
 32. Wulf A. Determining the Size and Shape of Gold Nanoparticles.” 2011.PhD [dissertation]. Carthage College; 2011.
 33. Mohammed YH, Sakrani SB, Rohani MS. Tunable morphological evolution of in situ gold catalysts mediated silicon nanoneedles. *Mater Sci Semicond Process.* 2016 Aug 1; 50: 36-42.
 34. Lidiawati D, Wahab AW, Karim A. Synthesis And Characterization Of Gold Nanoparticles Using Beluntas Leaf Extract *Pluchea indica*. *Indonesia Chim Acta.* 2019 May 30: 13-8.
 35. Khademi-Azandehi P, Moghaddam J. Green synthesis, characterization and physiological stability of gold nanoparticles from *Stachys lavandulifolia* Vahl extract. *Particuology.* 2015 Apr 1; 19: 22-6.
 36. Yang X, Dang Y, Lou J, Shao H, Jiang X. D-alanyl-D-alanine-modified gold nanoparticles form a broad-spectrum sensor for bacteria. *Theranostics.* 2018; 8(5): 1449.
 37. Ghaima KK, Saadedin SM, Jassim KA. Isolation, molecular identification and antimicrobial susceptibility of *Acinetobacter baumannii* isolated from Baghdad hospitals. *Int J Sci Res Publ.* 2015; 27: 31.
 38. Al Sehlawi ZS, Almohana AM, Al Thahab AA. Isolation and identification of *Acinetobacter baumannii* clinical isolates using novel methods. *J Babylon Univ.* 2014; 22(3): 1041-50.
 39. Shahzad S, Afzal M, Sikandar S. Chapter 1: Polymerase Chain Reaction. In: *Genetic Engineering- A Glimpse of Techniques and Applications.* 2020. p. 20–71
 40. Chen PZ, Gu FX. Gold nanoparticles for colorimetric detection of pathogens, *Ency. Biomed Eng.* 2018 Jan 1 : 108-115. Elsevier.
 41. He H, Dai J, Duan Z, Zheng B, Meng Y, Guo Y, et al. Unusual sequence length-dependent gold nanoparticles aggregation of the ssDNA sticky end and its application for enzyme-free and signal amplified colorimetric DNA detection, *Sci Rep.* 2016 Aug 1; 6(1): 1-7.

تطوير طريقة التحليل اللوني باستخدام الجسيمات النانوية من الذهب غير المعدلة لتحديد عزلات بكتريا *Acinetobacter baumannii* من عينات مختلفة

محمد موفق سحري¹ اماني محمد جسم² هناء ناجي عبدالله²

¹كلية التمريض ، جامعة تلغفر ، العراق.
²كلية التقنيات الصحية والطبية الجامعة التقنية الوسطى ، بغداد ، العراق.

الخلاصة:

تعد بكتريا *Acinetobacter baumannii* أحد المشاكل الصحية الخطيرة لكونها بكتيريا ذات مقاومة عالية للأدوية المتعددة لأغلب المضادات الحيوية المتاحة تجارياً. إن الهدف من هذه الدراسة هو تطوير طريقة التحليل اللوني للكشف الكمي عن الحامض النووي الهدف *DNA* لبكتريا *A. baumannii* بالاعتماد على جسيمات الذهب النانوية (AuNPs) من عينات مختلفة (الحروق والجروح والبلغم والدم والادرار) . تم جمع ستة وثلاثون عزلة بكتيرية *A. baumannii* من ثلاث مستشفيات في العراق من شهر أيلول 2020 الى شهر كانون الثاني 2021. تم إجراء العزل البكتيري والاختبارات الكيموحيوية متبوعة باستخلاص 36 عزلة من الحامض النووي *DNA* و 6 سلالات قياسية سالية ATCC (*Salmonalle typhi*, *Escherichia coli*, *Klebsiella pneumonia*, *Pseudomonas aeruginosa*, *Enterobacter aeruginosa*, *Staphylococcus aureus*) و سلالة موجبة ATCC واحدة تعود لبكتريا *A. baumannii* باستخدام طريقة الفينول/كلورفورم تم تصنيع AuNPs باستخدام طريقة اختزال السترات وفحصت بالـ XDR و FTIR و UV-VIS و FE-SEM و TEM. وظفت طريقة التحليل اللوني اعتماداً على جسيمات الذهب النانوية (الكروية) غير المعدلة. تم تضخيم بتقنية الـ PCR لتسلسل الجينوم للمنطقة الفاصلة *16S rRNA* (ITS) مع البادئ المستهدف المتخصص oligotargeters للحامض النووي *DNA*. أجري فحص واختيار *amplicon* الأفضل للبكتريا *A. baumannii* باستخدام جسيمات الذهب النانوية غير المعدلة AuNPs. إذ تمتلك AuNPs قابلية على كشف وتمييز بكتريا *A. baumannii* لونياً عن باقي السلالات الأخرى للبكتريا القياسية. وكان الوقت المستغرق لإجراء التحول لهذه العزلة القياسية حوالي 3 ساعات، بما في ذلك عمليتي إعداد العينة والتضخيم بحدود (0.025-1 ngul-1) كحد كسفي لتركيز الحامض النووي البكتيري. اثبتت كفاءة كشف التحلل اللوني لتشخيص عزلة *baumannii* بحساسية عالية وبساطة وقوة في التشخيص السريع لعزلات *A. baumannii* من عينات سريرية مختلفة

الكلمات المفتاحية: *Acinetobacter baumannii*، جسيمات الذهب النانوي، الفحص اللوني، *16S rRNA*، تفاعل البوليمراز المتسلسل